Prevention against diffuse spinal cord astrocytoma: can the Notch pathway be a novel treatment target?

Jian-jun Sun[1, *], Zhen-yu Wang[1], Ling-song Li[2], Hai-yan Yu[3], Yong-sheng Xu[3, 4], Hai-bo Wu[5], Yi Luo[1], Bin Liu[1], Mei Zheng[6], Jin-long Mao[7], Xiao-hui Lou[8, *]

1 Department of Neurosurgery, Peking University Third Hospital, Peking University, Beijing, China
2 China Stem Cell Research Center, Peking University Health Science Center, Peking University, Beijing, China
3 Clinical Stem Cell Center, Peking University Third Hospital, Peking University, Beijing, China
4 Clinical Laboratory of Tissue & Cell Research Center, Department of Biotech Treatment, Logistics College of Chinese People's Armed Police Force, Tianjin, China
5 Department of Neuroradiology, Peking University Third Hospital, Peking University, Beijing, China
6 Department of Neurology, Peking University Third Hospital, Peking University, Beijing, China
7 Neurosurgical Department, Peking Union Medical College Hospital, Beijing, China
8 Department of Neurosurgery, Rui'an People's Hospital, Wenzhou Medical University, Wenzhou, Zhejiang Province, China

Abstract

This study was designed to investigate whether the Notch pathway is involved in the development of diffuse spinal cord astrocytomas. BALB/c nude mice received injections of CD133+ and CD133− cell suspensions prepared using human recurrent diffuse spinal cord astrocytoma tissue through administration into the right parietal lobe. After 7–11 weeks, magnetic resonance imaging was performed weekly. Xenografts were observed on the surfaces of the brains of mice receiving the CD133+ cell suspension, and Notch-immunopositive expression was observed in the xenografts. By contrast, no xenografts appeared in the identical position on the surfaces of the brains of mice receiving the CD133− cell suspension, and Notch-immunopositive expression was hardly detected either. Hematoxylin-eosin staining and immunohistochemical staining revealed xenografts on the convex surfaces of the brains of mice that underwent CD133+ astrocytoma transplantation. Some sporadic astroglioma cells showed pseudopodium-like structures, which extended into the cerebral white matter. However, it should be emphasized that the subcortex xenograft with Notch-immunopositive expression was found in the fourth mouse received injection of CD133− astrocytoma cells. However, these findings suggest that the Notch pathway plays an important role in the formation of astrocytomas, and can be considered a novel treatment target for diffuse spinal cord astrocytoma.

Key Words: nerve regeneration; astrocytoma; mice; immunodeficiency (BALB/c) mice; Notch; nestin; glial fibrillary acidic protein; CD133; spinal cord; brain; MRI; neural regeneration

Introduction

Glioma is a type of tumor in the nervous system that originates from glial cells. It accounts for 30% of all tumors in the central nervous system (Goodenberger and Jenkins, 2012; Chen and Yakisich, 2014). Astrocytoma is the most common type of glioma, originating from astrocytes (Song et al., 2013). Diffuse astrocytoma, also named fibrillary astrocytoma, is a relatively low-grade astrocytoma with the ability to develop into higher-grade astrocytoma (Ranjan et al., 2011). Diffuse astrocytoma is most commonly found in children and young adults (Claes et al., 2007).

The cancer stem cell (CSC) hypothesis posits that only a subset of cells in a cancer is tumorigenic (Jiang and Uhrbom, 2012; Qiu et al., 2012; Zhao et al., 2013). These cells are sim-ilar to normal stem cells that can self-renew and differentiate into multiple types of cells in a cancer (Bao et al., 2006a; Wang et al., 2012, 2014; Wu, 2012). Several reports (Bao et al., 2006a; Beier et al., 2007; Shackleton et al., 2009; Jiang and Uhrbom, 2012; Yin et al., 2014) have demonstrated the existence of CSCs in brain gliomas. Emerging evidence (Bao et al., 2006b; Huse and Holland, 2009; Shackleton et al., 2009; Turchi et al., 2013) has shown that a small population of CSCs is responsible for long-term glioma propagation. CSCs are critical for the engraftment and long-term growth of gliomas (Bao et al., 2006b; Huse and Holland, 2009; Jiang et al., 2012; Najbauer et al., 2012; Fang et al., 2013; Liu et al., 2014).

A specific marker of glioma stem cells (GSCs) has been widely searched for, but the results have been inconclusive.

CD133 is the most widely used antigen for enrichment of GSCs (Yi et al., 2013; Liu et al., 2014), and has been repeatedly validated in freshly isolated patient specimens (Bao et al., 2006b; Wang et al., 2010). It is the consensus that GSCs have been prospectively enriched by selection of the CD133 cell surface marker (Beier et al., 2007; Shackleton et al., 2009; Liu et al., 2014). CD133 has been used as a GSC marker to identify and isolate a small fraction of cells in gliomas with a significantly increased potential to generate tumor neurospheres (Najbauer et al., 2012; Fang et al., 2013; Liu et al., 2014). However, several studies (Beier et al., 2007; Zhang et al., 2008; Son, 2009; Ivkovic et al., 2012; Noell et al., 2012) have found that CD133⁻ cells may still have the characteristics of GSCs, and that CD133 is not a unique marker for GSCs. Therefore, some authors (Eyler et al., 2008; Dasari et al., 2010; Fan et al., 2010; Muto et al., 2012; Fang et al., 2013) have suggested that CD133 should not be used as a unique marker for collecting glioma stem cells.

Notch activity is critically implicated in the radio resistance of GSCs (Wang, 2010). The Notch pathway can promote or repress tumorigenesis in a context-dependent manner (Azizidoost et al., 2014; Saito et al., 2014). The Notch pathway has functions in cell growth, proliferation, and survival (Chen et al., 2014a; Guichet et al., 2014). A new hypothesis was proposed by some scientists (Eyler et al., 2008; Dasari et al., 2010; Fan et al., 2010; Muto et al., 2012) that glioma cells would only become cancer stem cells if Notch is expressed, leading to sustained self-renewal and potent tumorigenicity, regardless of the expression of CD133 or other markers (Garner et al., 2013; Kristoffersen et al., 2013; Wu et al., 2013a).

Different sub-types of tumors may also have different markers for CSCs (Wieland et al., 2013; Wu et al., 2013b). Although many studies (Bao et al., 2006a; Son et al., 2009; Noell et al., 2012; Wieland et al., 2013) have investigated cell markers for GSCs in the brain, none (Furnari et al., 2007; Louis et al., 2007; Holmberg et al., 2011) have focused on GSCs isolated from recurrent spinal cord astrocytomas. In this study, we focused on identifying a marker for the isolation and generation of xenografts with a small population of original intramedullary diffuse spinal cord astrocytoma cells, and on the key role of the Notch pathway in the development of cerebral xenografts from only a few original spinal cord intramedullary astrocytoma cells.

Materials and Methods

Tissue collection and primary neurosphere culture
A tumor specimen was obtained from a patient with recurrent intramedullary diffuse spinal cord astrocytoma (MRI scan shown in **Figure 1**). The protocol for this study was approved by the Institutional Review Board of Peking University Medical Center, China. The patient and guardians provided written informed consent for surgical operation, medical photography and advanced basic research, as well as for publishing for the study.

Original astrocytoma cells were seeded at a density of 2,500 cells per cm^2 in chemically defined serum-free selection growth medium, consisting of basic fibroblast growth factor (bFGF; 20 ng/mL; Chemicon, Temecula, CA, USA),

epidermal growth factor (EGF; 20 ng/mL; Chemicon), and serum-free supplement (B27; Gibco, Grand Island, NY, USA, http://www.invitrogen.com) in a 3:1 mix of Dulbecco's modified Eagle's medium (DMEM; Sigma-Aldrich, St. Louis, MO, USA) and Ham's F-12 Nutrient Mixture (F12; Gibco, New York, NY, USA). The cultures were incubated at 37°C in a water-saturated atmosphere containing 5% CO_2. To maintain the undifferentiated state of neurosphere cultures, growth factors were replenished every 2 days. The growth state of the original astrocytoma cells was observed under an inverted microscope, twice per day. When tumor cells starve because of insufficient nutrition, a black center to the glioma neurosphere (as shown by the arrow in **Figure 2**) can be identified under the microscope, indicating that passage should be performed.

Flow cytometric analysis
Neurospheres were dissociated into a single cell suspension using Accutase (eBioscience). Cells were labeled for expression of CD133 according to the manufacturer's instructions (MiltenyiBiotec, Auburn, CA, USA) and analyzed on a FACSCalibur flow cytometer (BD Biosciences, Becton Dickinson, San Jose, CA, USA) with CellQuest software (Version 3.3, BD Biosciences, Becton Dickinson, San Jose, CA, USA). In brief, Fc receptors were blocked with blocking reagent and the cells were labeled by incubation with CD133-phycoerythrin (PE) monoclonal antibodies or isotype as a negative control, at 4°C for 10 minutes in the dark. Then, cells were washed and resuspended in 500 μL of wash buffer (PBS containing 0.5% bovine serum albumin and 2 mmol/L ethylenediaminetetraacetic acid). After acquisition, data were analyzed using CellQuest software. CD133⁺ cells were identified by the presence of the marker, which was set according to the isotype control.

Magnetic-activated cell sorting (MACS)
Tumors were dissociated into single cells using Accutase (eBioscience). Then, CD133⁺ cells were selected by magnetic bead sorting. Cells were incubated with CD133 antibodies conjugated to anti-biotin microbeads. CD133⁺ fractions were collected by eluting the MACS column. Purification of CD133⁺ cells from human gliomas by MACS can also allow for their isolation and growth. The culture condition for CD133⁺ cells was the same as for the original astrocytoma cells.

Establishment of tumor xenograft models
Original astrocytoma cells (1×10^4) in 5 μL of PBS were delivered into the right parietal lobe (0.5 μL/min) by stereotaxic injection through a glass electrode connected to a Hamilton syringe (Narishige, Tokyo). Stereotaxic coordinates, for injection into ten 4-week-old female BALB/c nude mice (Vital River Company, Beijing, China) were 2 mm lateral to the midline, 2 mm anterior to the coronal suture and 2 mm below the dura. All procedures were performed in accordance with Peking University Animal Care and Use Committee protocols. The original diffuse spinal cord astrocytoma cells were injected into the brains of immunodeficient

Figure 1 Recurrent intramedullary diffuse spinal cord astrocytoma 6 months after resection in a 42-year-old female suffering from lower extremity weakness and unsteady walk for 5 months.
The recurrent intramedullary tumor nodule (arrow) is shown on the MRI scan.
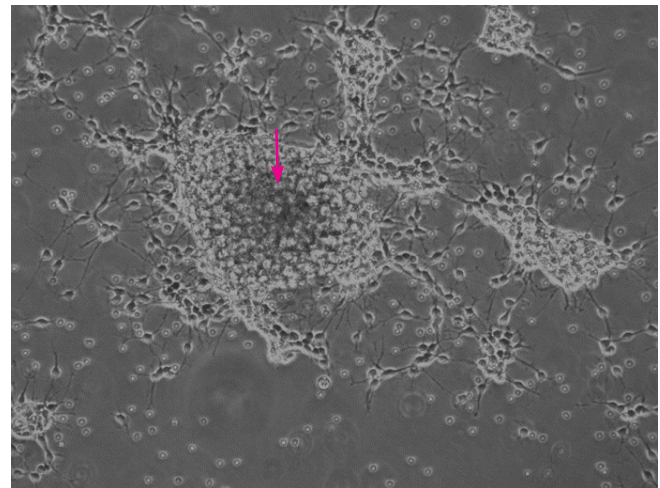

Figure 2 Primary astrocytoma neurosphere culture (inverted microscope).
When astrocytoma cells were starved because of insufficient nutrition, a black center to the astrocytoma neurosphere (arrow) can be identified, indicating that passage should be performed.
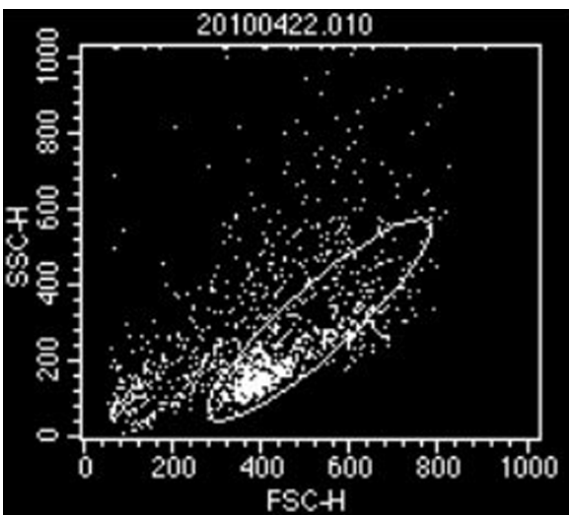

Figure 3 Identification of original astrocytoma cells.
Flow cytometric analyses showed that 49.44% of cells are the CD133$^+$ intramedullary diffuse spinal cord astrocytoma cell population.
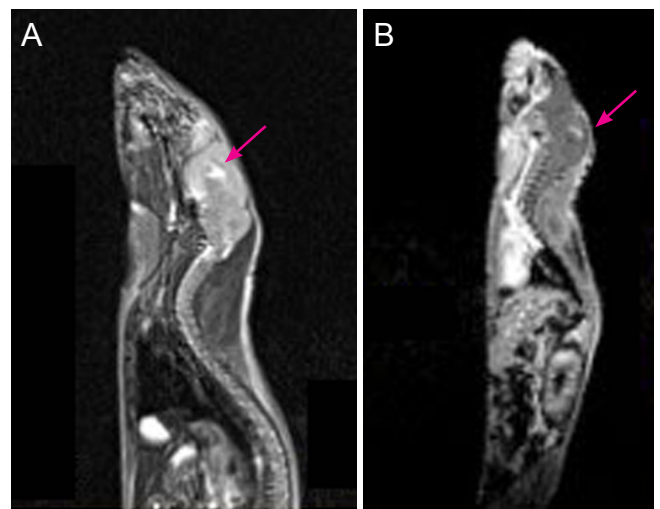

Figure 4 Cerebral tumor xenograft determined by MRI scans.
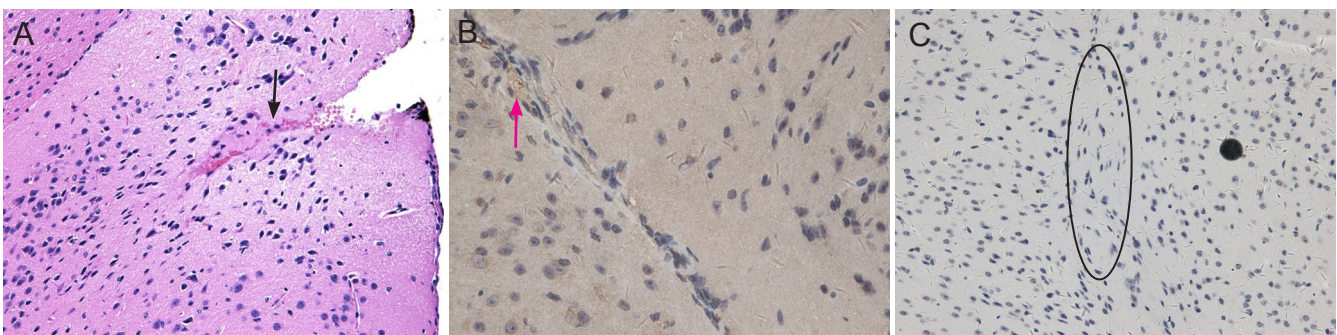(A, B) Cerebral tumor xenograft (arrows) on T2- and T1-weighted contrast images.

Figure 7 Histological changes to xenografts after transplantation of CD133$^-$ astrocytoma cells.
(A) At 10 weeks after transplantation of CD133$^-$ diffuse astrocytoma cells, an intra-cortex xenograft around the insertion site (arrow) was observed by hematoxylin-eosin staining. Original magnification: × 200. (B) Weak Notch immunoreactivity on partial cytoplasm and extracellular matrix of diffuse astrocytoma cells (arrow). Original magnification: × 400. (C) The xenograft cells showed negative immunoreactivity for CD133 (black circle). Original magnification: × 200.
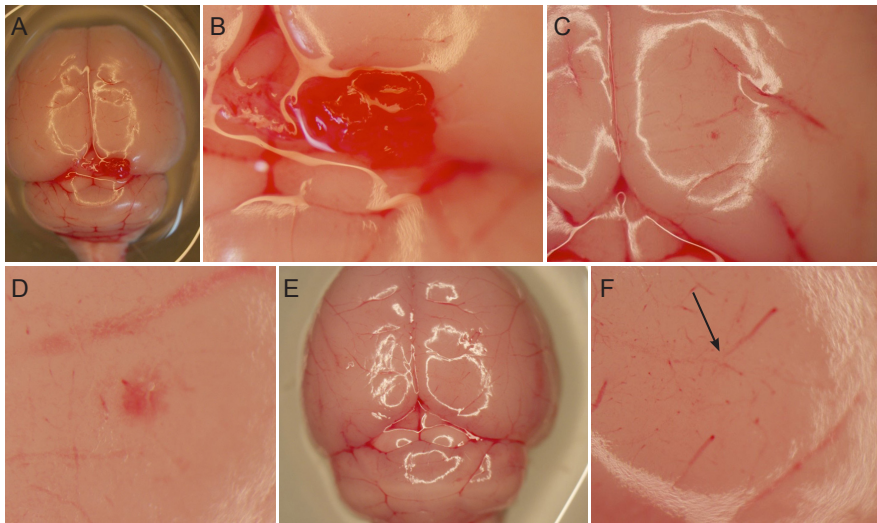
Figure 5 Gross changes of mouse brain after xenograft implantation.

(A, B) At 8 weeks after transplantation of CD133$^+$ cells, a red xenograft nodule was observed on the surface of one mouse brain. Original magnification: 4× (A) and 10× (B). (C, D) At 8 weeks after transplantation of CD133$^+$ cells, a red-brown lesion was observed on the cortex of another mouse brain, indicating the presence of a xenograft. Original magnification: 6× (C) and 10× (D). (E, F) At 10 weeks after transplantation of CD133$^-$ astrocytoma cells, a blurry insert needle spot (arrow) was left, without any abnormal lesions on the surface of the mouse brain. A xenograft was present in the subcortex. Original magnification: 6× (E) and 12× (F).
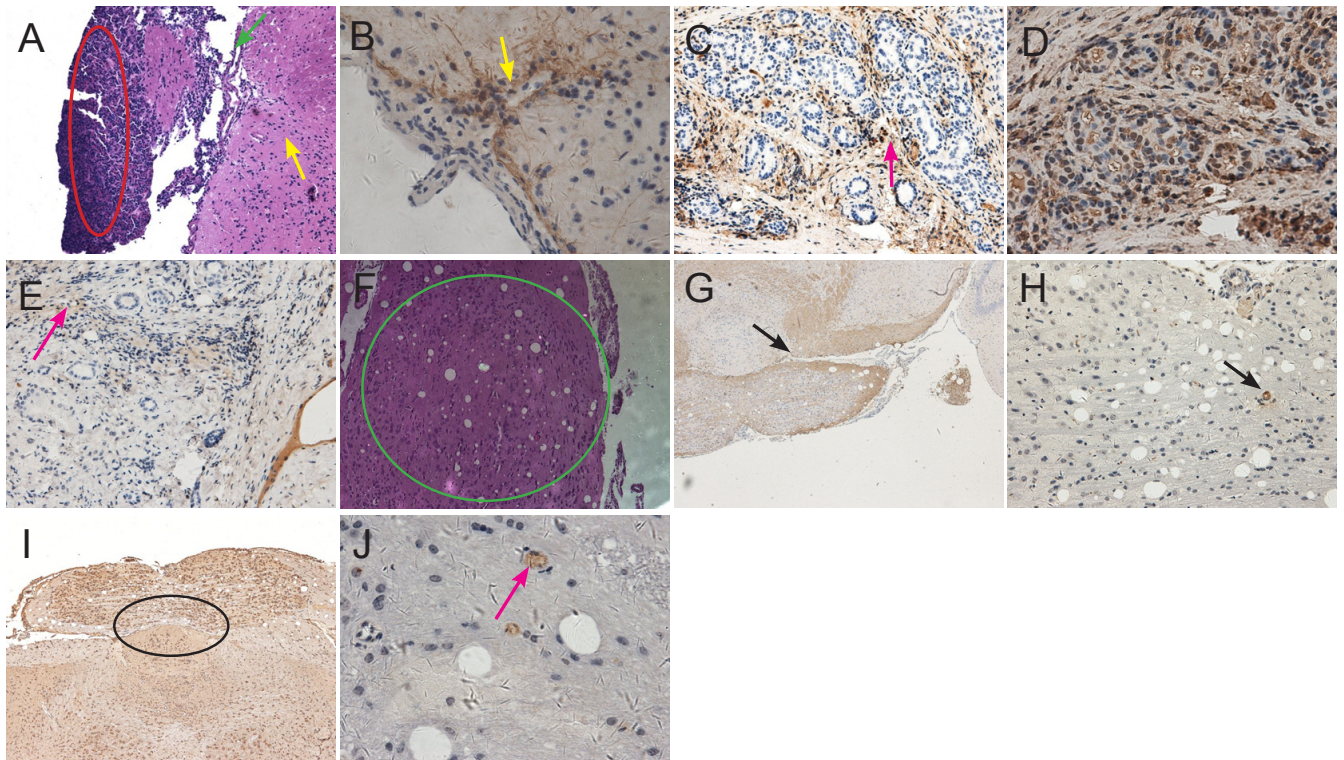

Figure 6 Histological changes to xenografts after transplantation of CD133$^+$ astrocytoma cells.

(A) At 8 weeks after cell transplantation, xenografts were observed outside the cerebral cortex of CD133$^+$ mice by hematoxylin-eosin staining. A large tumor nodule protrudes from the surface of cortex, in which there are atypical cells of different sizes (red oval circle). There are several vessels that supply blood to the tumor nodule in the juncture between the nodule and cortex (as shown by green arrows). Some diffuse astrocytoma cells like pseudopodia infiltrated the surrounding subcortical white matter (as shown by yellow arrows). Original magnification: × 100. (B) Many glioma cells on the surface of cortex of CD133$^+$ mouse showed strong GFAP-positive expression, several cells infiltrated deeply into the white matter (pointed by arrow). Original magnification: × 400. (C) Nestin immunoreactivity was seen in vascular cavity, wall, and extracellular matrix (arrow). Original magnification: × 200. (D) Strong Notch immunoreactivity was seen in the cell cytoplasm. Proliferating astrocytoma cells accumulating around the stem cell niche were observed on the same slide. Original magnification: × 400. (E) CD133 immunoreactivity was observed on the astrocytoma cell membrane (arrow). Original magnification: × 200. (F) At 11 weeks after transplantation of CD133$^+$ diffuse astrocytoma cells into mouse brain, a xenograft like a lotus root was found in the cortex (green circle). Original magnification: × 100. (G) GFAP immunoreactivity on the extracellular matrix of diffuse astrocytoma cells (arrow). Original magnification: × 40. (H) Nestin immunoreactivity on the pathological vascular cavity (arrow). Extracellular matrix infiltrated deep into the white matter, and a pathological vascular structure was seen inside the xenograft. Original magnification: × 100. (I) Cluster-like Notch immunoreactivity on the astrocytoma cell membrane and cytoplasm in the adjacent subcortex (black circle). Original magnification: × 100. (J) CD133 immunoreactivity was detected on the cell membrane of some scattered astrocytoma cells in a cell niche (arrow). Original magnification: × 400.

Table 1 Head circumference (cm) of mice receiving transplantation of CD133$^+$ and CD133$^-$ diffuse astrocytoma cells at different time points after cell transplantation

Time after transplantation (week)	CD133$^+$					CD133$^-$				
	1	2	3	4	5	1	2	3	4	5
1	4.6	4.5	4.95	4.8	5.1	5.1	4.6	4.9	4.5	5.0
2	4.7	5.0	4.9	5.4	4.9	4.9	5.0	5.1	5.1	4.9
3	4.8	4.9	5.1	5.4	4.9	4.8	5.1	4.9	5.2	4.9
4	5.0	5.1	5.2	Died	5.0	5.3	5.4	Died	5.2	5.2
5	5.1	5.2	5.4		5.6	5.3	5.0		5.1	5.6
6	5.1	5.4	5.6		5.3	5.6	5.3		5.4	5.0
7	5.1	5.6	5.3		Died	5.4	5.0		Died	5.1
8	5.0	5.3	5.5			5.4	5.5			5.7
9	5.5	5.3	Died			5.4	5.1			Died
10	5.1	5.4				5.5	5.1			
Mean ± SD	5.0±0.3	5.2±0.3	5.2±0.25	5.2±0.35	5.1±0.27	5.27±0.3	5.1±0.3	5.0±0.12	5.1±0.31	5.2±0.31

Table 2 Body mass (g) of mice receiving transplantation of CD133$^+$ and CD133$^-$ diffuse astrocytoma cells at different time points after cell transplantation

Time after transplantation (week)	CD133$^+$					CD133$^-$				
	1	2	3	4	5	1	2	3	4	5
1	20.3	23.3	24.5	20.0	21.9	20.9	18.1	19.8	15.1	19.2
2	22.4	25.6	25.4	23.3	24.2	23.1	22.3	22.5	16.5	23.7
3	23.5	26.4	26.6	22.9	24.0	22.9	21.9	23.1	16.2	23.4
4	23.2	27.4	27.3	24.2	25.2	24.6	23.1	23.6	18.1	24.6
5	23.5	26.2	26.0	23.4	24.6	23.6	22.6	22.6	17.3	25.2
6	23.0	25.7	26.6	Died	25.5	24.1	23.1	Died	17.2	25.2
7	23.5	26.9	27.8		25.6	24.5	24.3		18.3	25.0
8	24.1	27.8	29.0		Died	26.4	25.3		Died	26.6
9	25.1	28.1	27.9			25.1	24.3			25.4
10	24.9	28.3	Died			25.7	25.1			Died
11	24.7	28.5				26.8	25.1			
Mean ± SD	23.5±1.35	26.7±1.54	26.8±1.38	22.8±1.61	24.4±1.3	24.3±1.7	23.2±2.07	22.3±1.48	17±1.1	24.3±2.12

(BALB/c) mice. Then, the BALB/c mice were divided into a CD133$^+$ astrocytoma cell group and a CD133$^-$ astrocytoma cell group, with five mice in each group. Mice in the control group were injected with 5 μL of PBS. Head circumference and body mass of mice were measured twice per week after cell suspension or vehicle delivery.

MRI imaging

Xenografts were monitored by MRI scanning from 7 weeks after astrocytoma cell transplantation. A CD133$^+$ mouse and a CD133$^-$ mouse were scanned. MRI scans were performed on a 3.0-T MRI scanner (Siemens, Germany) with 50 mm diameter × 108 mm radio frequency (RF) rung-length small animal imaging coil (Litzcage small animal imaging system; Doty Scientific Inc., Columbia, SC, USA). Stereotaxic ear bars were used to minimize movement during the imaging procedure. After registering with a triplanar FLASH sequence, MRI studies were performed using fast spin echo T2- and pre T1-weighted MRI scans. An electrophysiological monitoring system was applied to monitor the electrocardiogram (ECG), respiration, and body temperature of mice during the whole procedure. The following parameters were used to acquire MRI scans: fast spin echo T2-weighted multi-echo (30, 60 ms) multi-slice sequences (1,000 ms; 256 × 256 matrix; 13–15 slices at 1 mm thick; 40 mm × 30 mm field of view, number of excitation = 4), and a T1-weighted multi-slice sequence (700/20 ms; 256 × 256 matrix; 13–15 slices at 1 mm thick, 40 mm × 30 mm field of view, number of excitation = 4). To determine the signal enhancement in the tumors, gadolinium-diethylenetriaminepentaacetic acid (Gd-DTPA 0.2 mmol/kg; Guerbet, Aulnay-sous-Bois, France) was intraperitoneally injected. Post contrast T1-weighted images were acquired using the above-mentioned T1-weighted image parameters.

Gross microscopic observation of mouse brain

Following anesthesia by intraperitoneal injection of Aldrich (0.2 mL/10 g), mice were sacrificed. The whole brains were taken out carefully under the microscope (SZM7045TR-B2, Lucky Zoom, Ningbo, Zhejiang Province, China). The outline, color and blood supplies on the cortex were observed.

Histological staining

After fixation in 4% formalin overnight, cerebral tissues were prepared into 5-μm-thick paraffin wax-embedded sections. Paraffin sections were deparaffinized and rehydrated. Sections were subjected to hematoxylin-eosin staining and immunohistochemical analysis. The dilutions and suppliers of primary antibodies used in this study were as follows: glial fibrillary acidic protein (GFAP; mouse, 1:2,000; Dako Denmark A/S, Glostrup, Denmark), nestin (mouse, 1:200; Merck Millipore, Darmstadt, Germany), CD133 (mouse, 1:1,000; MiltenyiBiotec), and Notch (mouse, 1:1,000; MiltenyiBiotec).

Stained tissues were analyzed by light microscope (BX-60, Olympus America Inc., Melville, NY, USA). Images were captured under an Olympus Color View digital camera. Sample preparation, histological staining and imaging process were all performed three times in the same manner.

Results

Identification of original astrocytoma cells

Among the original intramedullary diffuse spinal cord astrocytoma cells, 49.44% were CD133 positive (**Figure 3**). After identification by flow cytometric analyses, the original astrocytoma cells were continuously cultured.

Observation and measurement for mice receiving cell transplantation

At 7 and 11 weeks, one CD133$^+$ mouse and another CD133$^-$ mouse were selected to undergo daily MRI scans according to an obviously enlarged head circumference and fluctuated body mass. Head circumference showed a trend of rapid growth after cell transplantation and peaked at the 8th week. After 8 weeks, the head circumference showed a slight fluctuation. If the head circumference of any mouse receiving cell transplantation was obviously increased after 8 weeks (**Table 1**), the mouse underwent MRI and was sacrificed. The body mass of the mice receiving cell transplantation showed a trend toward a gradual increase, and most of them became stable in the later period (**Table 2**).

MRI scans

Xenografts were detected in every CD133$^+$ mouse. The xenografts were apparent in T2- and T1-contrast images (**Figure 4**). Xenografts were not observed in any CD133$^-$ mouse.

Gross observation of mouse brain

At 7–11 weeks after cell transplantation, a CD133$^+$ mouse and a CD133$^-$ mouse were sacrificed every week, with five pairs in total. Under the microscope, three CD133$^+$ mice showed a red xenograft nodule with abundant blood supply (**Figure 5A, B**) and two CD133$^+$ mice showed red-brown lesions on the brain surface around the insert spot (**Figure 5C, D**). With the exception of the 4th mouse with an implicated occupied lesion, the whole skulls and brain surfaces of the other CD133$^-$ mice were normal, with only the blurry insertion spot left (**Figure 5E, F**).

Histological changes in the xenografts

The xenografts were apparent by hematoxylin-eosin staining

in five mice receiving CD133$^+$ astrocytoma cells. At 8 weeks after cell transplantation, a convexity was seen outside the brains of mice receiving CD133$^+$ astrocytoma cells (**Figure 6A**). The xenografts looked like a lotus root and lay in the cortex, and partial glioma tissue infiltrated into the white matter (**Figure 6F−J**). Positive expression of GFAP, nestin, Notch and CD133 was detected in xenograft tissues in all CD133$^+$ mice (**Figure 6B−E, G−J**).

An intra-cortex xenograft around the insertion point was observed only in the fourth CD133$^-$ mouse brain after hematoxylin-eosin staining. Notch staining was positive, but CD133 staining was negative (**Figure 7A−C**). No xenograft tissues were observed in the brains of any other mouse receiving CD133$^-$ glioma cell transplantation. Only gliosis was detected in the brain of other mice in which both CD133 and Notch staining were negative. If only glioma cell xenografts were detected in hematoxylin-eosin staining, the xenograft showed positive expression for Notch in the same sequence tissue slice. However, not all xenografts showed positive expression for CD133 staining. The pathologic microvessels inside the glioma xenograft were observed on the same slides (**Figure 6C**, **H**).

Discussion

Whether CD133 or Notch can be considered a marker of GSCs remains inconclusive (Eyler et al., 2008; Dasari et al., 2010; Fan et al., 2010; Wang, 2010; Muto et al., 2012; Fang et al., 2013). We found that CD133$^-$ original astrocytoma cells formed xenografts in immune-deficient mouse brain. Moreover, the xenografts still showed negative expression for CD133 staining. However, all xenografts showed positive expression for Notch. It was hypothesized that Notch, but not CD133, played a key role in the formation of xenografts from the original diffuse spinal cord astrocytoma cells.

Current therapies for glioma include maximal surgical resection combined with radiotherapy and chemotherapy (Bao et al., 2006b; Furnari et al., 2007; Louis et al., 2007). Despite the significant toxicities of these therapies, most patients with nerve glioma suffer tumor recurrence owing to resistance to therapy (Bao et al., 2006b; Chen and Yakisich, 2014). The tumor regrowth and recurrence suggests that some tumor cells are resistant to therapy at treatment initiation. Because of invasion and infiltration into normal spinal cord white matter, diffuse astrocytoma frequently recurs and regrows as focal masses (Holmberg et al., 2011). Only a fraction of tumor cells are responsible for the recurrence and regrowth of diffuse astrocytoma (Ranjan et al., 2011). A crucial cellular subpopulation of GSCs was identified as having potent cancer stem cell activity (Chen et al., 2014; Wang, 2014), including sustained self-renewal abilities and being relatively resistant to radiotherapy (Bao et al., 2006b) and chemotherapy (Chen and Yakisich, 2014).

There is no consensus on how to select the subset of GSCs from original surgical glioma samples or what might represent a key marker for identifying GSCs (Alqudah et al., 2013; Turchi et al., 2013; Yin et al., 2014; Wieland et al., 2013). Bao et al. (2006b) considered that CD133$^+$ cancer cells contribute

to glioma radioresistance. However, CD133⁻ cells may still have characteristics of GSCs based on the fact that CD133⁻ cells can form tumors (Eyler et al., 2008; Zhang et al., 2008; Dasari et al., 2010; Ivkovic et al., 2012; Muto et al., 2012).

The definition of CSCs remains functional, requiring sustained self-renewal and tumor propagation (Jiang et al., 2012; Jin et al., 2012; Wang et al., 2014). In our study, the growth of astrocytoma xenografts was closely related to positive expression of Notch. The Notch pathway is a key signaling pathway for GSCs (Alqudah et al., 2013; Hu et al., 2014; Lagadec et al., 2014). Moreover, CD133⁺ is not a representative marker for GSCs. In addition, positive expression of Notch pathway might be correlated with the vitality of GSCs. Once Notch is expressed, regardless of the expression of CD133 or nestin, these astrocytoma cells are activated from the dormant state. These active glioma (astrocytoma) cells began to become active and proliferate, acting as truly functional GSCs (Hu et al., 2014; Lagadec et al., 2014; Saito et al., 2014).

Wang et al. (2010) demonstrated that the Notch signaling pathway plays an important role in the pathogenesis of glioma, and that these malignant brain tumors contained stem-like cancer cells with higher Notch activity. The Notch pathway represents a possible target in stem-like glioma cells, as several groups have shown that glioblastoma GSCs express Notch family genes (Alqudah et al., 2013; Hu et al., 2014; Lagadec et al., 2014). It is known that Notch regulates the self-renewal and differentiation of normal neural stem cells, and that GSCs share many characteristics with their normal cognates, including the signaling pathways that regulate self-renewal (Eyler et al., 2008; Zhang et al., 2008; Dasari et al., 2010; Wang et al., 2010; Muto et al., 2012). Several studies (Eyler et al., 2008; Zhang et al., 2008; Dasari et al., 2010; Ivkovic et al., 2012; Muto et al., 2012) have shown that the Notch pathway is critically involved in regulation of the radio-responsiveness of GSCs.

The usefulness of markers is only reliably apparent when evaluating freshly isolated patient specimens (Huse and Holland, 2009; Najbauer et al., 2012). CD133 and other cell surface markers are molecular interactors that mediate signals between cells and the microenvironment. Therefore, their expression and usefulness in GSC isolation may be missed if evaluated in culture environment *versus* a freshly dissociated tumor (Zhang et al., 2008; Dasari et al., 2010; Wang et al., 2010; Ivkovic et al., 2012). One study (Wang et al., 2010) reported that CD133⁻ cells in fresh specimens are able to grow tumors. These findings highlight the complexity of the CSC hypothesis as well as the field's appreciation that no single marker will be adequate to identify all GSC populations. Based on the results of our study, the Notch pathway might play a key role in the proliferation of GSCs and the formation of their microenvironment.

It is noted that the Notch signaling pathway mediates navigation for GSCs. A blocked Notch pathway partially interrupts the internal contact and results in temporary dormancy of GSCs (Hu et al., 2014; Lagadec et al., 2014). After temporary dormancy, the glioma cells can still proliferate into xenografts by activating the Notch signaling pathway (Garner et al., 2013). Blocking the Notch pathway partially suppresses the expression of CD133. Taken together, these findings suggest that Notch may play a particularly important role in promoting engraftment of GSCs and the long-term growth of gliomas. In summary, the Notch pathway plays an important role in the pathogenesis of diffuse spinal cord astrocytoma.

References

Alqudah MA, Agarwal S, Al-Keilani MS, Sibenaller ZA, Ryken TC, Assem M (2013) NOTCH3 is a prognostic factor that promotes glioma cell proliferation, migration and invasion via activation of CCND1 and EGFR. PLoS One 8:e77299.

Azizidoost S, Shanaki Bavarsad M, Shanaki Bavarsad M, Shahrabi S, Jaseb K, Rahim F, Shahjahani M, Saba F, Ghorbani M, Saki N (2014) The role of notch signaling in bone marrow niche. Hematology doi: http://dx.doi.org/10.1179/1607845414Y.0000000167.

Bao SD, Wu QL, Sathornsumetee S, Hao YL, Li ZZ, Hjielmeland AB, Shi Q, Mclendon RE, Bigner DD, Rich JN (2006a). Stem cell-like glioma cells promote tumor angiogenesis through vascular endothelial growth factor. Cancer Res 66:7843-7848.

Bao SD, Wu QL, Mclendon RE, Hao YL, Shi Q, Hjielmeland AB, Dewhirst MW, Bigner DD, Rich JN (2006b). Glioma stem cells promote radio resistance by preferential activation of the DNA damage response. Nature 444:756-760.

Beier D, Hau P, Proescholdt M, Lohmeier A, Wischhusen J, Oefner PJ, Aigner L, Brawanski A, Bogdahn U, Beier CP (2007) CD133(+) and CD133(-) glioblastoma-derived cancer stem cells show differential growth characteristics and molecular profiles. Cancer Res 67:4010-4015.

Chen G, Kong J, Tucker-Burden C, Anand M, Rong Y, Rahman F,Moreno CS, Van Meir EG, Hadjipanayis CG, Brat DJ (2014) Human brat Ortholog TRIM3 Is a tumor suppressor that regulates asymmetric cell division in glioblastoma. Cancer Res 74:4536-4548.

Chen J, Yakisich JS (2014) Editorial: emerging concepts and therapeutics strategies for the treatment of brain tumors. Anticancer Agents Med Chem 14:1063-1064.

Claes A, Idema AJ, Wesseling P (2007) Diffuse glioma growth: a guerilla war. Acta Neuropathol 114:443-458.

Dasari VR, Kaur K, Velpula KK, Guirati M, Fassett D, Klopfenstein JD, Dinh DH, Rao JS (2010) Upregulation of PTEN in glioma cells by cord blood mesenchymal stem cells inhibits migration via downregulation of the PI3K/Akt pathway. PLoS One 5:e10350.

Eyler CE, Foo WC, LaFiura KM, Mclendon RE, Hielmeland AB, Rich JN (2008) Brain cancer stem cells display preferential sensitivity to Akt inhibition. Stem Cells 26:3027-3036.

Fan X, Khaki L, Zhu TS, Soules ME, Talsma CE, Gul N, Koh C, Zhang J, Li YM, Maciaczyk J, Nikkhah G, Dimeco F, Piccirillo S, Vescovi AL, Eberhart CG (2010) Notch pathway blockade depletes CD133-positive glioblastoma cells and inhibits growth of tumor neurospheres and xenografts. Stem Cells 28:5-16.

Fang KM, Lin TC, Chan TC, Ma SZ, Tzou BC, Chang WR, Liu JJ, Chiou SH, Yang CS, Tzeng SF (2013) Enhanced cell growth and tumorigenicity of rat glioma cells by stable expression of human CD133 through multiple molecular actions. Glia 61:1402-1417.

Furnari FB, Fenton T, Bachoo RM, Mukasa A, Stommel JM, Stegh A, Hahn WC, Ligon KL, Louis DN, Brennan C, Chin L, DePinho RA, Cavenee WK (2007) Malignant astrocyticglioma: genetics, biology, and paths to treatment. Genes Dev 21:2683-2710.

Garner JM, Fan M, Yang CH, Du Z, Sims M, Davidoff AM, Pfeffer LM (2013). Constitutive activation of signal transducer and activator of transcription 3(STAT3) and nuclear factor κB signaling in glioblastoma cancer stem cellsregulates the Notch pathway. J Biol Chem 288:26167-26176.

Goodenberger ML, Jenkins RB (2012) Genetics of adult glioma. Cancer Genet 205:613-621.

Guichet PO, Guelfi S, Teigell M, Hoppe L, Bakalara N, Bauchet L, Duffau H, Lamszus K, Rothhut B, Hugnot JP (2014) Notch1 stimulation induces a vascularization switch with pericyte-like celldifferentiation of glioblastoma stem cells. Stem Cells doi: 10.1002/stem.1767.

Holmberg J, He X, Peredo I, Orrego A, Hesselager G, Xie K, Huang S (2011) Activation of neural and pluripotent stem cell signatures correlates with increased malignancy in human glioma. PLoS One 6:e18454.

Hu YY, Fu LA, Li SZ, Chen Y, Li JC, Han J, Liang L, Li L, Ji CC, Zheng MH, Han H (2014) Hif-1α and Hif-2α differentially regulate Notch signaling through competitive interaction with the intracellular domain of Notch receptors in glioma stem cells. Cancer Lett 349:67-76.

Huse JT, Holland EC (2009) Genetically engineered mouse models of brain cancer and the promise of preclinical testing. Brain Pathol 19:132-143.

Ivkovic S, Beadle C, Noticewala S, Massey SC, Swanson KR, Toro LN, Bresnick AR, Canoll P, Rosenfeld SS (2012) Direct inhibition of myosin II effectively blocks glioma invasion in the presence of multiple motogens. Mol Biol Cell 23:533-542.

Jiang X, Xing H, Kim TM, Jung Y, Huang W, Yang HW, Song S, Park PJ, CarrollRS, Johnson MD (2012) Numb regulates glioma stem cell fate and growth by altering epidermal growth factor receptor and Skp1-Cullin-F-box ubiquitin ligase activity. Stem Cells 30:1313-1326.

Jiang Y, Uhrbom L (2012) On the origin of glioma. Ups J Med Sci 117:113-121.

Jin X, Kim SH, Jeon HM, Beck S, Sohn YW, Yin J, Kim JK, Lim YC, Lee JH, Kim SH, Kang SH, Pian X, Song MS, Park JB, Chae YS, Chung YG, Lee SH, Choi YJ, Nam DH, Choi YK, et al. (2012) Interferon regulatory factor 7 regulates glioma stem cells via interleukin-6 and Notch signalling. Brain 135:1055-1069.

Kristoffersen K, Villingshøj M, Poulsen HS, Stockhausen MT (2013) Level of Notch activation determines the effect on growth and stem cell-likefeatures in glioblastoma multiforme neurosphere cultures. Cancer Biol Ther 14:625-637.

Lagadec C, Vlashi E, Frohnen P, Alhiyari Y, Chan M, Pajonk F (2014) The RNA-binding protein Musashi-1 regulates proteasome subunit expression inbreast cancer- and glioma-initiating cells. Stem Cells 32:135-144.

Liu M, Inoue K, Leng T, Guo S, Xiong ZG (2014) TRPM7 channels regulate glioma stem cell through STAT3 and Notch signaling pathways. Cell Signal 26:2773-2781.

Louis DN, Ohgaki H, Wiestler OD, Cavenee WK, Burger PC, Jouvet A, Scheithauer BW, Kleihues P (2007) The 2007 WHO classification of tumours of the central nervous system. Acta Neuropathol 114:97-109.

Muto J, Imai T, Ogawa D, Nishimoto Y, Okada Y, Mabuchi Y, Kawase T, Iwanami A, Mischel PS, Saya H, Yoshida K, Matsuzaki Y, Okano H (2012) RNA-binding protein musashi1 modulates glioma cell growth through the post-transcriptional regulation of Notch and PI3 Kinase/Akt signaling pathways. PLoS One 7:e33431.

Najbauer J, Huszthy PC, Barish ME, Garcia E, Metz MZ, Myers SM, Gutova M, Frank RT, Miletic H, Kendall SE, Glackin CA, Bjerkvig R, Aboody KS (2012) Cellular host responses to gliomas. PLoS One 7:e35150.

Noell S, Ritz R, Wolburg-Buchholz K, Wolburg H, Fallier-Becker P (2012) An allograft glioma model reveals the dependence of aquaporin-4 expression on the brain microenvironment. PLoS One 7:e36555.

Qiu S, Tan XH, Huang H (2012) Progress in the source and surface markers of brain tumor stem cells. Zhongguo Zuzhi Gongcheng Yanjiu 16:1095-1098.

Ranjan M, Santosh V, Tandon A, Anandh B, Sampath S, Devi BI, Chandramouli BA (2011) Factors predicting progression of low-grade diffusely infiltrating astrocytoma. Neurol India 59:248-253.

Saito N, Fu J, Zheng S, Yao J, Wang S, Liu DD, Yuan Y, Sulman EP, Lang FF, Colman H, Verhaak RG, Yung WK, Koul D (2014) A high Notch pathway activation predicts response to γ secretase inhibitors inproneural subtype of glioma tumor-initiating cells. Stem Cells 32:301-312.

Shackleton M, Quintana E, Fearon ER, Morrison SJ (2009) Heterogeneity in cancer: cancer stem cells versus clonal evolution. Cell 138:822-829.

Son MI, Woolard K, Nam DH, Lee J, Fine HA (2009) SSEA-a is an enrichment marker for tumor-initiating cells in human glioblastoma. Cell Stem Cell 4:440-452.

Song XB, Yang ZY, Deng XL, Wang XP, Zhang SP, Huang J, Zhang XK (2013) In vitro isolation, culture and identification of brain tumor stem cells from human astrogliomas. Zhongguo Zuzhi Gongcheng Yanjiu 17:56-61.

Turchi L, Debruyne DN, Almairac F, Virolle V, Fareh M, Neirijnck Y, Burel-Vandenbos F, Paquis P, Junier MP, Van Obberghen-Schilling E, Chneiweiss H, Virolle T (2013) Tumorigenic potential of miR-18A in glioma initiating cells requires NOTCH-1signaling. Stem Cells 31:1252-1265.

Wang H, Sun T, Hu J, Zhang R, Rao Y, Wang S, Chen R, McLendon RE, Friedman AH, Keir ST, Bigner DD, Li QJ, Wang H, Wang XF (2014) miR-33a promotes glioma-initiating cell self-renewal via PKA and NOTCH pathways. J Clin Invest doi: 10.1172/JCI75284.

Wang JL, Wakeman TP, Lathia JD, Hjelmeland AB, Wang XE, White RR, Rich JN, Sullenger BA (2010) Notch promotes radio resistance of glioma stem cells. Stem Cells 28:17-28.

Wang XX, Liu JP (2012) Research progress in brain tumor stem cells. Zhongguo Zuzhi Gongcheng Yanjiu 16:2637-2640.

Wieland A, Trageser D, Gogolok S, Reinartz R, Höfer H, Keller M, Leinhaas A,Schelle R, Normann S, Klaas L, Waha A, Koch P, Fimmers R, Pietsch T, Yachnis AT, Pincus DW, Steindler DA, Brüstle O, Simon M, Glas M, et al. (2013) Anticancer effects of niclosamide in human glioblastoma. Clin Cancer Res 19:4124-4136.

Wu J, Ji Z, Liu H, Liu Y, Han D, Shi C, Wang C, Yang G, Chen X, Shen C,Li H, Bi Y, Zhang D, Zhao S (2013a) Arsenic trioxide depletes cancer stem-like cells and inhibits repopulation ofneurosphere derived from glioblastoma by downregulation of Notch pathway. Toxicol Lett 220:61-69.

Wu N, Lin X, Zhao X, Zheng L, Xiao L, Liu J, Ge L, Cao S (2013b) MiR-125b acts as an oncogene in glioblastoma cells and inhibits cell apoptosis through p53 and p38MAPK-independent pathways. Br J Cancer 109:2853-2863.

Wu W (2012) Effect of Wnt/β-Catenin signal pathway adjusted by suppressor of cytokine signaling 3 on tumor stem cells and its application in treatment of glioblastoma multiforme. Zhongguo Zuzhi Gongcheng Yanjiu 16:5988-5992.

Yi F, Ma J, Ni W, Chang R, Liu W, Han X, Pan D, Liu X, Qiu J (2013) The top cited articles on glioma stem cells in Web of Science. Neural Regen Res 8:1431-1438.

Yin J, Park G, Lee JE, Park JY, Kim TH, Kim YJ, Lee SH, Yoo H, Kim JH, Park JB (2014) CPEB1 modulates differentiation of glioma stem cells via downregulation of HES1 and SIRT1 expression. Oncotarget 5:6756-6769.

Zhang Y, Zhang N, Dai B, Liu M, Sawaya R, Xie K, Huang S (2008) FoxM1B transcriptionally regulates vascular endothelial growth factor expression and promotes the angiogenesis and growth of glioma cells. Cancer Res 68:8733-8742.

Zhao ZF, Fan RT, Yang Y, Sun JR, Hu X, Eileen S, Yang B (2013) In vitro radiosensitivity of brain cancer stem cells in brain glioma. Zhongguo Zuzhi Gongcheng Yanjiu 17:3455-3460.